Band structure and optical gain of tensile-strained germanium based on a 30 band k·p formalism

Moustafa El Kurdi, Guy Fishman, Sébastien Sauvage, and Philippe Boucaud[a)]
Institut d'Electronique Fondamentale, CNRS-Univ Paris-Sud 11, Bâtiment 220, 91405 Orsay, France

(Received 19 October 2009; accepted 20 November 2009; published online 13 January 2010)

We have investigated the band structure of tensile-strained germanium using a 30 band **k·p** formalism. This multiband formalism allows to simultaneously describe the valence and conduction bands, including the *L*, Δ, and Γ valleys. We calculate the energy band variation as a function of strain and obtain that the crossover from indirect to direct band gap occurs for a tensile in-plane strain of 1.9%. The effective masses of density of states are deduced from the calculated conduction and valence band density of states. Significant deviations are observed as compared to the effective masses of density of states values of unstrained bulk germanium. We finally calculate the optical gain that can be achieved with tensile-strained bulk germanium. An optical gain larger than 3000 cm^{-1} is predicted for a carrier density of 1×10^{18} cm^{-3} and a 3% in-plane biaxial strain. This optical gain is larger than the one of GaAs calculated with the same formalism and is much larger than the experimental free-carrier absorption losses. This gain should be sufficient to achieve lasing in these structures. © *2010 American Institute of Physics*. [doi:10.1063/1.3279307]

I. INTRODUCTION

Bulk germanium is an indirect band gap semiconductor. However, the energy band structure is strongly dependent on the lattice deformation. A transition from indirect to direct band gap has been predicted for tensile-strained germanium since the energy position of the conduction Γ valley versus strain decreases more rapidly than the band-edge *L* valley.[1,2] Uniaxial tension along the [111] direction can also lead to a direct band gap.[3] A direct band gap is of particular importance for light emission and to achieve population inversion. Its occurrence would be very promising for the demonstration of a germanium laser and the development of germanium and silicon photonics. Tensile-strained germanium can be obtained by different techniques. A small tensile strain (0.2%) can be introduced by growing germanium on a silicon substrate because of the difference in thermal expansion coefficient between the germanium layer and the substrate.[4] Optical gain has been recently evidenced in germanium at room temperature by combining this small tensile strain with a strong *n*-doping.[5] The growth of Ge on GeSiSn was proposed by Menendez and co-workers.[6] This approach could provide tensile strain of a few percent which might be sufficient to obtain a direct band gap. A theoretical gain calculation for quantum well lasers has been developed in Ref. 7 for this heterosystem. Growth on III-V semiconductors is also an option.[8] However, the prediction of a direct band gap, as reported in Ref. 1, does not imply that a significant optical gain can be achieved. One needs to take into account the density of states beyond the parabolic dispersion in order to accurately calculate the optical gain between valence and conduction bands and to compare this optical gain with the free-carrier absorption losses. The purpose of this work is to provide the calculation of the band structure of tensile-strained germanium and to demonstrate that high optical gain can be achieved with this material.

We have developed a band structure calculation of tensile-strained germanium using a 30 band **k·p** formalism. The 30 band **k·p** formalism is known to provide an accurate description of the valence and conduction bands all over the Brillouin zone.[9–11] It is therefore an appropriate formalism to describe simultaneously the Γ, Δ, *L*, heavy-hole (hh), and light-hole (lh) bands and their dependences as a function of strain. The band structures of strained SiGe and strained Ge layers deposited on SiGe buffers were also calculated using a 30 band formalism in Ref. 12. Only compressively strained germanium can be achieved in the case of strain imposed by SiGe buffers. Here, we concentrate on the specific case of tensile-strained germanium and on its optical properties. We obtain that the transition from indirect to direct band gap occurs for a tensile deformation of 1.9%. The corresponding low-temperature energy band gap is 530 meV (2.34 μm wavelength). We calculate the valence and conduction density of states for unstrained and strained germanium using the 30 band formalism. It provides the values of the effective masses of density of states which are significantly different from those of bulk unstrained germanium. We finally calculate the interband optical gain as a function of the carrier density and show that optical gains higher than 3000 cm^{-1} could be obtained for a 1×10^{18} cm^{-3} carrier density and a 3% tensile strain. These optical gains are compared to those calculated on bulk GaAs using the same formalism.

II. 30 BAND K·P FORMALISM AND GERMANIUM BAND STRUCTURE

A. Parametrization

The 30 band **k·p** formalism was introduced following the approach described in Refs. 9–11. The strain is taken into

[a)]Electronic mail: philippe.boucaud@ief.u-psud.fr. URL: http://pages.ief.u-psud.fr/QDgroup.

TABLE I. Parameters (in eV) used in the 30 band $\mathbf{k}\cdot\mathbf{p}$ formalism. a, b, c, and d correspond to Refs. 21, 33, 23, and 27, respectively. According to formulas (1)–(9), a value of $b_{\Gamma_5^+}$ with a minus sign must be considered while a positive value of this parameter must be taken into account according to the notations presented in Ref. 14.

$a_{\Gamma_2^-}-a_{\Gamma_5^+}$	$a_{\Gamma_4^-}-a_{\Gamma_5^+}$	$b_{\Gamma_4^-}$	$b_{\Gamma_5^+}$	$\left[\Xi_d+\frac{1}{3}\Xi_u-a_{\Gamma_5^+}\right]^L$	$\left[\Xi_d+\frac{1}{3}\Xi_u-a_{\Gamma_5^+}\right]^\Delta$	$a_{\Gamma_{1u}^+}-a_{\Gamma_5^+}$
−9.75 (a)	−3.9 (b)	−5.1	−2.55 (c)	−3.6 (d)	−0.9	5.3

account through the Bir–Pikus Hamiltonian.[13,14] A (001) biaxial strain has two contributions on the band structure: a hydrostatic component which shifts the band gap energy and a uniaxial component which splits the bands by lowering the symmetries. The effect of strain on the energy band positions can also be calculated through the following formulas[13] using Koster's notations for symmetry elements in the simple group.[9,15] For the indirect conduction valleys, the following equations were first expressed in Refs. 16 and 17. For the valence band, the strain induced shift taking into account the spin orbit and strain splitting interaction was expressed in Refs. 18 and 19,

$$\Delta E_c^\Gamma = a_{\Gamma_2^-}\varepsilon, \tag{1}$$

$$\Delta E_c^L = \left[\Xi_d + \frac{1}{3}\Xi_u - a_{\Gamma_5^+}\right]^L \varepsilon, \tag{2}$$

$$\Delta E_{\Delta_2} = \left[\Xi_d + \frac{1}{3}\Xi_u - a_{\Gamma_5^+}\right]^\Delta \varepsilon + \frac{2}{3}\Xi_u^\Delta(\varepsilon_\perp - \varepsilon_\parallel), \tag{3}$$

$$\Delta E_{\Delta_4} = \left[\Xi_d + \frac{1}{3}\Xi_u - a_{\Gamma_5^+}\right]^\Delta \varepsilon - \frac{1}{3}\Xi_u^\Delta(\varepsilon_\perp - \varepsilon_\parallel), \tag{4}$$

$$\Delta E_{\Delta_4} - \Delta E_{\Delta_2} = -\Xi_u^\Delta(\varepsilon_\perp - \varepsilon_\parallel), \tag{5}$$

$$\Delta E_h = a_{\Gamma_5^+}\varepsilon, \tag{6}$$

$$\delta E_v = 2b_{\Gamma_5^+}(\varepsilon_\perp - \varepsilon_\parallel), \tag{7}$$

$$\Delta E_v^{\mathrm{lh}} = \frac{-\Delta_0}{3} + \Delta E_h + \Delta E_s^{\mathrm{lh}}, \tag{8}$$

$$\Delta E_s^{\mathrm{lh}} = \frac{-\Delta_0}{6} + \frac{\delta E_v}{4} + \frac{1}{2}\left(\Delta_0^2 + \Delta_0\delta E_v + \frac{9}{4}\delta E_v^2\right)^{1/2}, \tag{9}$$

where $\varepsilon=\varepsilon_{xx}+\varepsilon_{yy}+\varepsilon_{zz}$, $\varepsilon_\parallel=\varepsilon_{xx}=\varepsilon_{yy}=(a_\parallel-a_{\mathrm{Ge}})/a_{\mathrm{Ge}}$, $\varepsilon_\perp=\varepsilon_{zz}=(a_\perp-a_{\mathrm{Ge}})/a_{\mathrm{Ge}}$, a_{Ge} being the lattice parameter of bulk germanium, and $a_\parallel$ and $a_\perp$ being the in-plane and out-of-plane lattice parameters of strained germanium. For a biaxial deformation considered in the following, $\varepsilon_\perp=-(2C_{12}/C_{11})\varepsilon_\parallel$, where C_{12} and C_{11} are the elastic constants (49.4 and 131.5 GPa at low temperature, respectively).[20] ΔE_c^Γ and ΔE_c^L correspond to the shift of the Γ_2^- and L conduction bands. ΔE_{Δ_2} and ΔE_{Δ_4} correspond to the energy shift of the Δ_2 and Δ_4 conduction valleys. ΔE_h is the mean energy shift of the valence band extrema at $\mathbf{k}=0$. δE_v is the linear splitting versus uniaxial strain between hh and lh for a null spin-orbit interaction. ΔE_v^{lh} corresponds to the energy shift of the lh band in the case of a tensile strain with respect to an energy origin taken at the lh and hh extrema without strain. It corresponds to a mixing of lh and spin-orbit states due to strain coupling. For simplicity, we denote it as the lh band. ΔE_s^{lh} is similar to ΔE_v^{lh} but with respect to a different energy origin, namely, the mean energy of the three valence bands which is shifted by $-\Delta_0/3$ from the top lh and hh band extrema without strain. Δ_0 is the spin-orbit splitting (0.29 eV for germanium).[21] Note that there are two main limits to the treatment of the strain effect. First, we use a model with the elastic "constants" considered as constants, i.e., we do not take into account the nonlinearities of elastic constants which can be observed at very large deformations. It is justified since the considered deformations are only of a few percent. Second, the introduction of strain in the $\mathbf{k}\cdot\mathbf{p}$ matrix leads to nondiagonal terms of the form $Pk(1+\varepsilon)$, where P is a matrix element. We have neglected the terms $Pk\varepsilon$, an approximation which is valid as long as ε is small as compared to 1. As long as there are uncertainties on the values of the P term which can be as large as $\pm 10\%$ depending on semiconductors, neglecting the $Pk\varepsilon$ terms is legitimate for ε values of few percent.

The main parameters used in the $\mathbf{k}\cdot\mathbf{p}$ calculation are given in Table I. $a_{\Gamma_5^+}$ is set equal to zero since only the difference between the parameters has to be considered. Several parameters which are introduced in the $\mathbf{k}\cdot\mathbf{p}$ matrix have a strong influence on the energy band positions. The notation of the following parameters corresponds to the one used in Ref. 11. $a_{\Gamma_2^-}$ controls the hydrostatic dependence of the Γ conduction band. It has also some influence on the position of the L valley. $b_{\Gamma_4^-}$ controls the splitting of the p-conduction band and has a strong influence on the splitting of the Δ valley. We have chosen the value of $b_{\Gamma_4^-}$ equal to −5.1 eV because it leads to a Δ valley splitting which is in agreement with the value that can be calculated from Eq. (5) and a band potential parameter Ξ_u^Δ of 9.75 eV as reported by nonlocal empirical pseudopotentials.[22] This value of Ξ_u^Δ is consistent with other values of Ξ_u^Δ reported in literature (9.42 eV in Ref. 23, 10.2 eV in Ref. 24). The adjustment of $b_{\Gamma_4^-}$, based on the Δ valley splitting, is more appropriate than the adjustment of this parameter from the interband band gap of SiGe alloys, as done in Ref. 11, which led to a −9.5 eV value for germanium. The Δ valley is usually not considered when the band gap of tensile-strained germanium is calculated. However, it is intrinsically included in the 30 band formalism. For a compressively strained germanium layer, the Δ valley is split into Δ_4 and Δ_2 valleys and the Δ_4 valley represents the minimum. The Δ_4 valley has a weak dependence on the in-plane strain while the Δ_2 valley has a strong dependence on strain. For tensile-strained germanium, it is the opposite: The Δ_2 valley represents the minimum and its energy strongly decreases when the strain increases. Note that if the $b_{\Gamma_4^-}$ pa-

rameter is large (−6.8 eV and above in absolute value), the Δ valley splitting becomes important and the energy of the Δ valley becomes lower than the energy of the L and Γ valleys. In this case, the tensile-strained germanium cannot become a direct band gap semiconductor.

In literature on 20 or 30 band $\mathbf{k}\cdot\mathbf{p}$ modeling,[11,25] the strain is usually taken into account through the Bir–Pikus Hamiltonian. This Hamiltonian only describes the strain interaction between 14 bands. This restriction was mainly due to the lack of knowledge of the strain parameters for the other bands than the standard 14 bands. The use of a truncated basis of interaction for a strain Hamiltonian did nonetheless provide a satisfactory description of the band structure since the considered strain magnitudes were weak.[11,25] However, the band-edge states, especially at the Brillouin zone edge, are significantly mixed with the other bands outside the 14 band bases.[26] As an example, we can consider the L valley of unstrained germanium. The L_1 state at the Brillouin zone edge in the [111] direction, which is associated with the L band edge, is a mixture composed of 5.4% of the valence band states (Γ_5^+), 31.2% of p-conduction bands (Γ_4^-) and 31.4% of s-conduction band Γ_2^-, which are the bands usually included in the Bir–Pikus Hamiltonian when strain is considered. However, the L_1 state also has non-negligible components, typically 18%, with the Γ_{1u}^+ band which is the second s-like conduction band. For the Δ state, the same feature can be observed with Γ_{1u}^+ components reaching 36%. In the following, we argue that the introduction of the interaction of this Γ_{1u}^+ band into the strain Hamiltonian can provide a better description of the L valley of germanium under strain in agreement with experimental findings.

Despite the lack of knowledge for the strain potential parameters of the high-energy bands, we can adjust these parameters to correctly fit the L and Δ valley strain potentials. The most important strain effect is the one which influences the L valley. An experimental value was reported in Ref. 27 for the strain potential of the L valley [Eq. (2)] $\left[\Xi_d+\frac{1}{3}\Xi_u-a_{\Gamma_5^+}\right]^L=-3.6$ eV. This value was used in the calculations of Ref. 6. We note that this hydrostatic dependence is lower than the one of the direct band gap energy $a_{\Gamma_2^-}-a_{\Gamma_5^+}=-9.75$ eV and explains the direct band gap formation under tensile strain. The hydrostatic potential value for the Γ_{1u}^+ band is adjusted to $a_{\Gamma_{1u}^+}-a_{\Gamma_5^+}=5.3$ eV in order to obtain a good agreement between the energy shift of the conduction L valley calculated with the $\mathbf{k}\cdot\mathbf{p}$ formalism and the value obtained by Eq. (2) and the value of $\left[\Xi_d+\frac{1}{3}\Xi_u-a_{\Gamma_5^+}\right]^L$ reported in the experiments of Ref. 27.

We emphasize that there are two distinct ways to calculate the influence of strain: formulas (1)–(9) describe the effect of strain on the energy of the bands at specific points in the reciprocal space; the Bir–Pikus Hamiltonian introduced in the 30 band formalism provides a description of the influence of strain on the whole band structure. Some input parameters of the $\mathbf{k}\cdot\mathbf{p}$ formalism are adjusted in order to obtain a good agreement between values calculated with the $\mathbf{k}\cdot\mathbf{p}$ formalism and energy changes estimated at specific Brillouin zone points following formulas (1)–(9) using experimental or theoretical deformation potentials. As shown below, a comparison between both methods makes sense since as the $\mathbf{k}\cdot\mathbf{p}$ formalism describes the interaction between all the bands, a change in parameters might influence the position of different bands, not only the band with the most direct link.

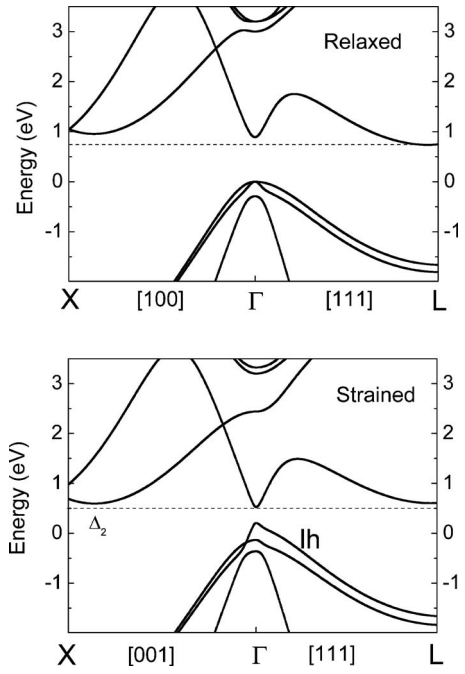

FIG. 1. Low temperature bulk Ge band structure (top) and band structure of 3% in-plane tensile-strained germanium (bottom). The dashed line highlights the minimum of the conduction band.

B. Band structure

Figure 1 shows a comparison between the bulk germanium band structure and the band structure of tensile-strained germanium. For bulk Ge, the band gap is indirect with the minimum of the conduction band at the L valley in the [111] direction. At low temperature, the indirect band gap energy of Ge related to the L valley is 736 meV while the direct band gap energy is 890 meV. Thus, there is only a relatively small difference of 154 meV between both values. At room temperature, the corresponding indirect hole-L and direct hole-Γ band gap energies are 664 and 800 meV, respectively. The key feature associated with the tensile strain is the different energy dependences versus strain of the L valley and of the zone center Γ valley. Under tensile strain, the energy of the Γ valley decreases more rapidly than the energy of the L valley. This is explained by the larger strain potential for the Γ valley as compared to the L valley since both valleys shift according to Eqs. (1) and (2). Thus, there is a transition between the indirect and direct band gaps. This effect is illustrated in Fig. 1 (bottom), which shows the calculated band structure for a 3% tensile strain. The minimum of the conduction band is at the zone center Γ valley, which indicates that the material has a direct band gap. Meanwhile, the degeneracy at zone center of the valence band is lifted and the valence band maximum corresponds to the lh subband.

Figure 2 shows the energy dependence of the Γ, Δ_2, L, and lh extrema as a function of the in-plane biaxial strain. The energy reference is taken at the hh-lh maximum without

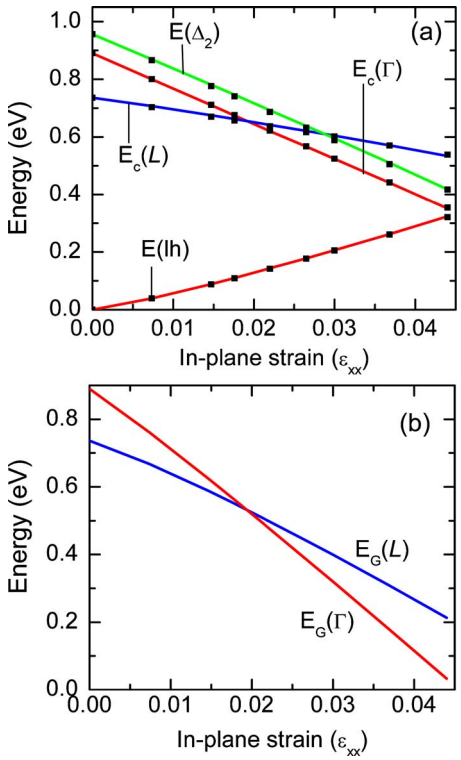

FIG. 2. (Color online) (a) Energy dependence at low temperature (4 K) of the Γ, Δ_2, *L*, and lh extrema as a function of the in-plane biaxial strain. The lines correspond to the results given by the $\mathbf{k}\cdot\mathbf{p}$ formalism. The squares correspond to the predictions given by formulas (1)–(9). (b) Variations of the direct band gap energy $E_G(\Gamma)=E_c(\Gamma)-E(\mathrm{lh})$ and of the *L* band gap $E_G(L)=E_c(L)-E(\mathrm{lh})$. The curves corresponding to $E_c(\Gamma)$ and $E_c(L)$ cross for an in-plane strain of 1.9%, which indicates the transition from indirect to direct band gap.

deformation. The values are calculated at low temperature. The symbols correspond to the band gap variations, as estimated by formulas (1)–(9). A good agreement is obtained between the 30 band formalism and the calculations of the band variations following formulas (1)–(9). As shown below, the main interest of the 30 band $\mathbf{k}\cdot\mathbf{p}$ formalism is to provide an accurate description of the density of states. The energy of the conduction bands decreases as the in-plane strain is increased. The striking feature is the difference in slopes between the *L*, Δ, and Γ valleys while the Δ_2 valley remains at about 70 meV above the Γ valley. The *L* valley has a weaker dependence (−44 meV/% in-plane strain) than the Γ valley (−121 meV/% in-plane strain) and a transition from indirect to direct band gap occurs for an in-plane strain of 1.9%. This value is in good agreement with 1.8% and 2% values reported for these transitions in Refs. 2 and 4. The energy of the lh band increases when the in-plane strain increases while the energy of the hh band decreases. The lh band energy shift leads to an additional decrease in the energy gap. Thus, a small tensile strain variation has a strong impact on the band gap variation. At the crossover between indirect and direct band gaps, the low-temperature band gap energy is 530 meV corresponding to a 2.34 μm wavelength. The variation of the direct energy band gap as a function of strain is also shown in Fig. 2. This variation can be interpolated with a good approximation by a linear dependence $E_G(\Gamma)=0.89-20\times\varepsilon_{\parallel}$ (eV). The band gap is predicted to reach zero for an in-plane strain of 4.5%.

C. Effective masses

We have calculated the equienergy surfaces of the Γ, Δ, *L*, and lh bands for relaxed and tensile-strained germanium (not shown here). The equienergy surfaces are calculated at 20 meV away from the maximum band edge. A significant difference between these equienergy surface shapes is observed when the in-plane biaxial strain is present. It indicates that the effective mass tensor of strained germanium differs significantly from the one of bulk Ge. We note that the effective mass tensor can be used in a simplified approach to calculate the band structure and the optical properties, but this approach is only valid near the band extrema. Only a multiband calculation can provide an accurate description of the equienergy surfaces. However, it is interesting to extract some effective mass parameters from this modeling which could be useful for, e.g., quantum well calculations. These values are summarized in Table II. The calculated effective masses of the Γ (0.039 m_0, where m_0 is the free electron mass) and lh valleys (0.0435 m_0) of bulk Ge are in good agreement with the experimental values of 0.038 and 0.043–0.0438 reported in Refs. 20 and 21. For the *L* valley, the calculated values of 1.60 m_0 for $m_{\parallel}^L$ and 0.085 m_0 for $m_{\perp}^L$

TABLE II. Effective masses and effective masses of density of states corresponding to the different valleys of relaxed and strained germanium. The "strained" part refers to 3% tensile-strained germanium. The masses are given in units of m_0. m_{xx}, m_{yy}, and m_{zz} correspond to the effective masses along the [100], [010], and [001] directions. $m_{\parallel}$ and $m_{\perp}$ correspond to effective masses parallel or perpendicular to the valley direction. For Δ_2, $m_{zz}=m_{\parallel}$. For the *L* valley in strained germanium, $m_{\perp}$ is given for the [−110] direction; this value depends on the considered perpendicular direction. m_{DOS} corresponds to the values obtained by the multiband calculation by fitting the local density of states for each valley following Eq. (11).

	Relaxed				Strained			
Direct valleys		m_{xx}, m_{yy}	m_{zz}	m_{DOS}		m_{xx}, m_{yy}	m_{zz}	m_{DOS}
Γ_c		0.039	0.039	0.039		0.03	0.015	0.025
Γ_{lh}		0.0435	0.0435	0.05		0.143	0.015	0.079
Indirect valleys	$m_{\parallel}$	$m_{\perp}$	m_{zz}	m_{DOS}	$m_{\parallel}$	$m_{\perp}$	m_{zz}	m_{DOS}
Δ_2	0.93	0.195	0.93	1.16	0.80	0.19	0.80	0.49
L	1.60	0.085	0.13	0.60	2.30	0.067	0.094	0.55

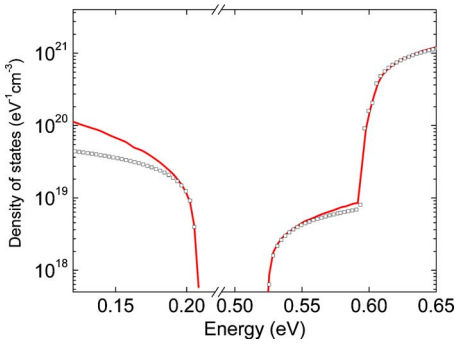

FIG. 3. (Color online) Density of states of a 3% in-plane tensile-strained germanium (full line). The density of states obtained for parabolic dispersions and fitted effective masses of density of states as reported in Table II [Eq. (11)] are shown with squares. The energy band gap is 320 meV. The vertical axis is in log scale.

are also in good agreement with the experimental values of 1.59 m_0 and 0.0823 m_0 reported in Refs. 20 and 21. If we consider the z direction for strained Ge, the effective mass of the L valley is $m_{zz}^{L}=0.094\ m_0$, which is six times larger than the zone center effective mass of the conduction band $m_{zz}^{\Gamma}=0.015\ m_0$. For the Δ_2 valley, the effective mass along z is $m_{zz}^{\Delta_2}=m_{\|}^{\Delta_2}=0.80\ m_0$. Consequently, in presence of quantum confinement along the z direction, as the band edge energy differences are only 70 meV (80 meV) between Δ_2 (L valley) and Γ, a large energy quantization could change a direct band gap material into fundamental indirect band gap quantum wells.

The effective masses of density of states are critical parameters and are frequently used to estimate the threshold of lasers.[28] In a first approximation and by considering only two directions in the case of multivalley anisotropic bands such as the L and Δ valleys, we have

$$\overline{m_{\mathrm{DOS}}^{L,\Delta}}=M_{L,\Delta}^{2/3}(m_{\perp}^{2}m_{\|})^{1/3}, \tag{10}$$

where $m_{\perp}$ and $m_{\|}$ are the effective mass perpendicular and parallel to the valley direction i.e. [111] for L and [001] for Δ_2, and M is the number of equivalent directions. $M_L=4$ is not changed with biaxial strain while $M_{\Delta}=6$ is changed into $M_{\Delta_2}=2$ and $M_{\Delta_4}=4$ under biaxial strain. A better estimation of the effective masses of density of states can be deduced from the density of states calculated with the 30 band formalism. The density of states is evaluated from the band diagram calculation in discretized k-space, which is obtained by considering Born–Von Karman boundary conditions. The electronic wavevector is written as eigenstates of a finite crystal volume V, i.e., $\mathbf{k}=(2\pi/L)(N_x,N_y,N_z)$, where N_x, N_y, and N_z are integers and L^3 is the crystal volume. For integration purposes, we have considered a volume of $(1500\ a)^3$, where a is the crystal lattice parameter. The density of states is obtained by counting the states in a small energy window. The effective mass of density of states is then defined and obtained by fitting the density of states integrated over all directions with m_{DOS} following a parabolic band law

$$g(E)=\frac{\sqrt{2}}{\pi^2\hbar^3}(m_{\mathrm{DOS}})^{3/2}\sqrt{E}. \tag{11}$$

Figure 3 shows the example of the calculated density of states for 3% tensile-strained germanium. For relaxed and strained germanium, the effective masses of density of states, which are deduced from Eq. (11) and the $\mathbf{k}\cdot\mathbf{p}$ calculation, are presented in Table II. For L and Δ_2 valleys, the effective masses of density of states are consistent with the expression $\overline{m_{\mathrm{DOS}}^{L,\Delta}}$ given by Eq. (10) estimated with the transverse and longitudinal masses calculated by $\mathbf{k}\cdot\mathbf{p}$ theory (0.57 m_0 for m_{DOS}^{L} and 1.08 m_0 for $m_{\mathrm{DOS}}^{\Delta}$). For a 3% tensile-strained germanium, the effective masses of density of states are $m_{\mathrm{DOS}}^{\Gamma}=0.025\ m_0$, $m_{\mathrm{DOS}}^{\Delta_2}=0.49\ m_0$, $m_{\mathrm{DOS}}^{L}=0.55\ m_0$, and $m_{\mathrm{DOS}}^{\mathrm{lh}}=0.079\ m_0$ for Γ, Δ_2, L, and lh bands, respectively.

Despite a strong nonparabolicity of the band dispersion for both L and Δ_2, especially in the longitudinal direction when strain is present, there is no significant deviation from the parabolic law given by Eq. (11) for energies close to the band edge within 20 meV (60) for the Δ_2 (L) valleys. As seen in Fig. 3, the same feature is true for the lh band for energies within 10 meV from the band edge. There is indeed a good overlap between the full line corresponding to the density of states calculated from the band diagram dispersion and the squares which are obtained from the parabolic law given by Eq. (11) using $m_{\mathrm{DOS}}^{\mathrm{lh}}=0.079\ m_0$. However, the deviation from the parabolic law becomes significant at 10 meV below the valence band edge. These deviations from parabolic law have an impact on the calculation of the optical gain since the latter one is directly related to band filling statistics for the material under nonequilibrium carrier injection. The deviation from the parabolic law is even more significant for the gain calculation at very high carrier densities.

III. GAIN CALCULATION

In the following, we use the band diagram calculated from the 30 band model to evaluate the optical gain of strained germanium. First, we extract the joined density of states for zone center valence and conduction bands as a function of vertical (in k-space) optical transition energy. The contribution of the optical indirect transitions are neglected, but the indirect valleys are accounted for in the calculation of the conduction quasi-Fermi levels E_{f_c} and E_{f_v}. We use the density of states, as shown in Fig. 3, to evaluate E_{f_c} and E_{f_v}. For the case of a 10^{18} cm^{-3} carrier density under a 3% biaxial strain, the conduction quasi-Fermi level is $E_{f_c}=78$ meV above the direct conduction band edge instead of 128 meV when considering only the zone center band.

The optical gain of the germanium layer is calculated from the absorption spectrum

$$\alpha(\hbar\omega)=C_0\rho_j(\hbar\omega)\int|\langle u_i|\boldsymbol{\varepsilon}\cdot\mathbf{p}|u_f\rangle|^2\frac{d\Omega}{4\pi}, \tag{12}$$

where $C_0=\pi e^2/cn\varepsilon_0 m_0^2\omega$. $\boldsymbol{\varepsilon}$ is the polarization of the incident light. $\rho_j(\hbar\omega)$ is the joined density of states for the conduction band and valence bands in the presence of carriers. It corresponds to the density of direct transitions at energy $\hbar\omega$. It is obtained by using the calculated band dispersion deduced from the $\mathbf{k}\cdot\mathbf{p}$ formalism following $\rho_j(\hbar\omega)=(2/V)\Sigma_{\mathbf{k}}\delta[E_c^{\Gamma}(\mathbf{k})-E_{\mathrm{lh}}(\mathbf{k})-\hbar\omega]\{f_v[E_{\mathrm{lh}}(\mathbf{k})]-f_c[E_c^{\Gamma}(\mathbf{k})]\}$, where f_v and f_c are the Fermi–Dirac distributions for the valence band and the conduction band, respec-

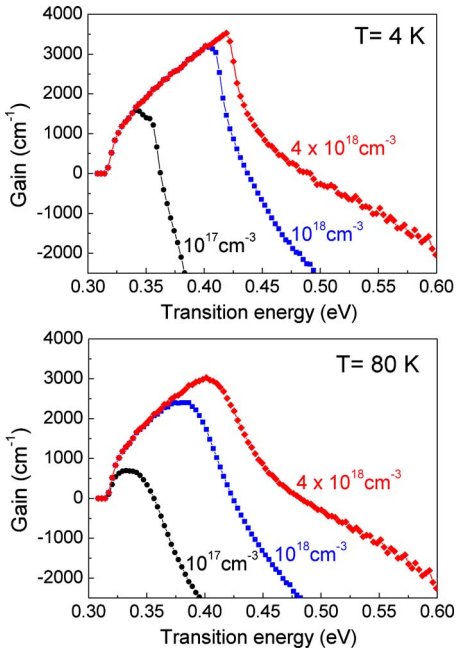

FIG. 4. (Color online) 4 (top) and 80 K (bottom) optical gain for a 3% tensile-strained germanium. Three carrier densities are depicted (10^{17}, 10^{18}, and 4×10^{18} cm^{-3}).

tively. The quasi-Fermi levels are calculated for strained material from the density of states following $N=\int_{E_c^{\Gamma}(0)}^{\infty}\rho_c(E)f_c(E)dE$ and $P=\int_{E_{\mathrm{lh}}(0)}^{\infty}\rho_v(E)f_v(E)dE$ with $N=P$. The averaged square of the interband dipolar momentum $\int|\langle u_i|\boldsymbol{\varepsilon}\cdot\mathbf{p}|u_f\rangle|^2(d\Omega/4\pi)$ is calculated by using the momentum matrix element of the $\mathbf{k}\cdot\mathbf{p}$ Hamiltonian $\langle u_i|\boldsymbol{\varepsilon}\cdot\mathbf{p}|u_f\rangle=(m_0/\hbar)\langle u_i|\boldsymbol{\varepsilon}\cdot\nabla_k H|u_f\rangle$, where u_i and u_f are the zone center lh and conduction band states. In the absorption calculation, we use the matrix element of zone center transitions, which is, in good approximation, weakly dependent on k in the k-space considered range. The vertical transitions considered in the absorption calculation involve conduction and valence band states at $k<5\%$ of the $2\pi/a$ Brillouin zone. The average value of $|\langle u_i|\boldsymbol{\varepsilon}\cdot\mathbf{p}|u_f\rangle|^2$ is obtained by its integration over a 4π solid angle with the incident polarization $\boldsymbol{\varepsilon}=\cos\varphi\sin\theta\mathbf{e_x}+\sin\varphi\sin\theta\mathbf{e_y}+\cos\theta\mathbf{e_z}$, where θ varies between 0 and π and φ varies between 0 and 2π.

The calculation of the optical gain shown in Fig. 4 does not account for broadening mechanisms. As discussed below, these predicted values of optical gain are compared to those of GaAs calculated with the same formalism. If we account for the broadening, the amplitude of the optical gain will be decreased and the amplitude of the decrease will depend on the exact value of the broadening. More particularly, the changes can be important when the spectral range of the gain is of the order of the broadening, which is not expected at high carrier densities.

Figure 4 shows the calculated gain at 4 K (top) and at 80 K (bottom) for a tensile-strained germanium with a 3% in-plane deformation. The calculated gain is shown as a function of the interband transition energy for three different carrier densities (10^{17}, 10^{18}, and 4×10^{18} cm^{-3}). At 4 K, the optical gain reaches a value of 3170 (3500) cm^{-1} at an energy of 405 (420) meV for an injected carrier density of 10^{18} cm^{-3} (4×10^{18} cm^{-3}). At 80 K, the gain reaches 2500 cm^{-1} for a 10^{18} cm^{-3} carrier density. Note that the 3500 cm^{-1} gain value calculated at 4 K only decreases to 2900 cm^{-1} when the Dirac delta function used in the calculation of the joined density of states is replaced by a Lorentzian with a 10 meV broadening. For a broadening value of 40 meV, the gain is still as large as 1900 cm^{-1}. These gain values are large and can be compared to the intrinsic losses associated with free-carrier absorption. We have used the empirical value of free-carrier absorption of Ref. 28, which has been obtained by fitting the experimental data reported in Refs. 29 and 30,

$$\alpha=-3.4\times10^{-25}N\lambda^{2.25}-3.2\times10^{-25}P\lambda^{2.43}, \tag{13}$$

where N and P are the electron and hole densities in cm^{-3}, λ is the wavelength in units of nanometer, and α is in units of cm^{-1}. For an energy of 405 meV, i.e., 3.06 μm wavelength, the free-carrier absorption is around 120 cm^{-1} for a 10^{18} cm^{-3} carrier density. Thus, there is a significant net gain for tensile-strained germanium at a moderate injected carrier density. This optical gain could be used to achieve lasing in standard ridge waveguides or using photonic crystal resonators as cavities.[31,32] These predicted gain values can be compared to the ones predicted for bulk GaAs even if the resonance wavelength differs. At low temperature, the theoretical gain in GaAs reaches 2500 cm^{-1} for a 10^{18} cm^{-3} carrier density. For this carrier density, the spectral width of the gain is significantly smaller for GaAs (48 meV) as compared to strained germanium (80 meV). At 10^{17} cm^{-3}, the gain is only 250 cm^{-1} for GaAs whereas the gain is around 1500 cm^{-1} for strained germanium. This is due to the fact that the transparency is achieved at much lower carrier density for strained germanium. First, the effective masses of strained germanium are much smaller than for GaAs; second, the strain lifts the degeneracy of the hole bands and the minimum is given by the lh band for strained germanium. These features reinforce the interest for strained germanium. Note that a thorough comparison between GaAs and strained Ge should take into account the broadening values associated with these materials. A systematic study of the gain as a function of broadening, temperature, and carrier density is beyond the scope of this article.

IV. CONCLUSION

We have investigated the band structure of relaxed and tensile-strained germanium using a 30 band $\mathbf{k}\cdot\mathbf{p}$ formalism. A transition from indirect to direct band gap is found to occur for a 1.9% in-plane tensile strain. The 30 band $\mathbf{k}\cdot\mathbf{p}$ formalism provides an accurate description of the density of states of the strained material. This feature is particularly important since the dispersion relation is strongly nonparabolic. We have deduced the effective masses of density of states from the density of states obtained by the 30 band $\mathbf{k}\cdot\mathbf{p}$ formalism. Finally, we have calculated the optical gain that could be achieved with tensile-strained germanium. A strong optical gain is predicted and should be sufficient to achieve lasing under optical or electrical injection with this material.

ACKNOWLEDGMENTS

This work was partly supported by the French Ministry of Industry under the Nano2012 convention and by RTRA Triangle de la Physique. We thank Daniel Bensahel for his support and fruitful discussions.

[1]R. Soref, J. Kouvetakis, and J. Menendez, Mater. Res. Soc. Symp. Proc. **958**, 13 (2007).
[2]R. Soref, J. Kouvetakis, J. Tolle, J. Menendez, and V. D'Costa, J. Mater. Res. **22**, 3281 (2007).
[3]F. Zhang, V. H. Crespi, and P. Zhang, Phys. Rev. Lett. **102**, 156401 (2009).
[4]Y. Ishikawa, K. Wada, D. D. Cannon, J. Liu, H.-C. Luan, and L. C. Kimerling, Appl. Phys. Lett. **82**, 2044 (2003).
[5]J. Liu, X. Sun, L. C. Kimerling, and J. Michel, Opt. Lett. **34**, 1738 (2009).
[6]J. Menéndez and J. Kouvetakis, Appl. Phys. Lett. **85**, 1175 (2004).
[7]S.-W. Chang and S. L. Chuang, IEEE J. Quantum Electron. **43**, 249 (2007).
[8]Y. Bai, K. E. Lee, C. Cheng, M. L. Lee, and E. A. Fitzgerald, J. Appl. Phys. **104**, 084518 (2008).
[9]S. Richard, F. Aniel, and G. Fishman, Phys. Rev. B **70**, 235204 (2004).
[10]S. Richard, F. Aniel, and G. Fishman, Phys. Rev. B **72**, 245316 (2005).
[11]M. El Kurdi, S. Sauvage, G. Fishman, and P. Boucaud, Phys. Rev. B **73**, 195327 (2006).
[12]D. Rideau, M. Feraille, L. Ciampolini, M. Minondo, C. Tavernier, H. Jaouen, and A. Ghetti, Phys. Rev. B **74**, 195208 (2006).
[13]G. Bir and G. Pikus, *Symmetry and Strain-Induced Effects in Semiconductors* (Wiley, New York, 1974).
[14]M. El Kurdi, G. Fishman, S. Sauvage, and P. Boucaud, Phys. Rev. B **68**, 165333 (2003).
[15]G. F. Koster, J. O. Dimmock, R. G. Wheeler, and H. Satz, *Properties of the Thirty-Two Point Groups* (MIT, Cambridge, MA, 1963).
[16]C. Herring and E. Vogt, Phys. Rev. **101**, 944 (1956).
[17]I. Balslev, Phys. Rev. **143**, 636 (1966).
[18]F. H. Pollak and M. Cardona, Phys. Rev. **172**, 816 (1968).
[19]C. G. Van de Walle, Phys. Rev. B **39**, 1871 (1989).
[20]O. Madelung, *Semiconductors: Data Handbook*, 3rd ed. (Springer, Berlin, 1984).
[21]H. H. Landolt and R. Börnstein, *Physics of Group IV Elements and Group III-V Compounds*, Landolt-Börnstein, New Series, Group III Vol. 17a (Springer, Berlin, 1982).
[22]M. V. Fischetti and S. E. Laux, J. Appl. Phys. **80**, 2234 (1996).
[23]C. G. Van de Walle and R. M. Martin, Phys. Rev. B **34**, 5621 (1986).
[24]M. M. Rieger and P. Vogl, Phys. Rev. B **48**, 14276 (1993).
[25]S. Richard, F. Aniel, G. Fishman, and N. Cavassilas, J. Appl. Phys. **94**, 1795 (2003).
[26]M. Cardona and F. H. Pollak, Phys. Rev. **142**, 530 (1966).
[27]C. N. Ahmad and A. R. Adams, Phys. Rev. B **34**, 2319 (1986).
[28]J. Liu, X. Sun, D. Pan, X. Wang, L. C. Kimerling, T. L. Koch, and J. Michel, Opt. Express **15**, 11272 (2007).
[29]W. G. Spitzer, F. A. Trumbore, and R. A. Logan, J. Appl. Phys. **32**, 1822 (1961).
[30]R. Newman and W. W. Tyler, Phys. Rev. **105**, 885 (1957).
[31]M. El Kurdi, S. David, X. Checoury, G. Fishman, P. Boucaud, O. Kermarrec, D. Bensahel, and B. Ghyselen, Opt. Commun. **281**, 846 (2008).
[32]T.-P. Ngo, M. El Kurdi, X. Checoury, P. Boucaud, J. F. Damlencourt, O. Kermarrec, and D. Bensahel, Appl. Phys. Lett. **93**, 241112 (2008).
[33]A. Blacha, H. Presting, and M. Cardona, Phys. Status Solidi B **126**, 11 (1984).